Journal of Biological Physics **30:** 345–364, 2004.

Cell Movements and Mechanical Force Distribution During the Migration of *Dictyostelium* Slugs

JEAN-PAUL RIEU[1,*], CATHERINE BARENTIN[1], SATOSHI SAWAI[2], YASUO MAEDA[3] and YASUJI SAWADA[4]

[1]*Laboratoire de Physique de la Matière Condensée et des Nanostructures,Université Claude Bernard Lyon I and CNRS, 43 Boulevard du 11 Novembre 1918, 69622 Villeurbanne Cedex, France;* [2]*Graduate School of Information Sciences, Tohoku University, 2-1-1 Katahira, Aoba-ku, Sendai 980-77, Japan;* [3]*Department of Developmental Biology and Neurosciences, Graduate School of Life Sciences, Tohoku University, Aoba, Sendai 980-8578, Japan;* [4]*Tohoku Institute of Technology, 35-1 Yagiyama-Kasumi, Taihaku, 983, Sendai, Japan*

*(*Author for correspondence, e-mail: rieu@lpmcn.univ-lyon1.fr)*

Abstract. Migration of *Dictyostelium discoideum* slugs results from coordinated movement of their constituent cells. It is generally assumed that each cell contributes to the total motive force of the slug. However, the basic mechanisms by which mechanical forces (traction and resistive forces) are transmitted to the substrate, their magnitude and their location, are largely unknown. In this work, we performed detailed observations of cell movements by fluorescence microscopy using two-dimensional (2D) slugs. We show that 2D slugs share most of the properties of 3D ones. In particular, waves of movement propagate in long 2D slugs, and slug speed correlates with slug length as found in 3D slugs. We also present the first measurements of the distribution of forces exerted by 2D and 3D slugs using the elastic substrate method. Traction forces are mainly exerted in the central region of the slug. The large perpendicular forces around slug boundary and the existence of parallel resistive forces in the tip and/or the tail suggest an important role of the sheath in the transmission of forces to the substrate.

Key words: *Dictyostelium* slug, elastic substrate, wave of movement, traction force, slime sheath

1. Introduction

The cellular slime mould *Dictyostelium discoideum* provides an experimentally accessible and simple model system to investigate many biological processes including chemotaxis, cell signaling and coordinated cell movements within cellular aggregates [1]. Although molecular details are still unknown, it is assumed that chemotactic waves organize the aggregation of free living single amoebae and the cell movements in multicellular aggregates including slugs [2]. There is a characteristic pattern of cell movement in *Dictyostelium* slugs: cells in the anterior prestalk

zone show vigorous rotational movement around the central core of the tip, while cells in the prespore zone move straight forward in the direction of slug migration in a periodic fashion along the slug axis [3–5]. Periodic motion and optical waves with the same period have been observed in slugs of many *Dictyostelium* strains [6].

Siegert and Weijer [3] proposed that the prestalk cell movement is organised by a rotating scroll wave of cAMP, which serves as pacemaker for the formation of planar cAMP waves, which in turn direct periodic forward movement of prespore cells. According to the authors, prestalk cells do not contribute to slug migration, since the tip is often raised above the substratum. Only prespore cells propel the slug forward due to their close contact to the substratum and the surrounding slime sheath [5]. On the other hand, earlier studies suggested that the more active anterior cells pull the posterior ones [7–9].

The aim of this work is to clarify the exact mechanism of slug motion by performing detailed quantitative observations of individual cell motion and direct measurements of mechanical forces exerted by the cells during slug migration. We are particularly interested in understanding how and where the forces are transmitted to the substrate. To measure forces, we recorded the deformations of elastic substrates with fluorescent beads embedded inside. Complex calculations are necessary to convert the deformation field in force field [10–11]. Elastic substrate experiments so far have been only performed on single cells like fibroblasts or keratocytes [12], never on multicellular systems such as migrating slugs. Recently, deformation of nonwrinkling silicone substrates exerted by single amoebae was visualized, and forces were estimated using a simple calibration [13].

We report here experimental results on two-dimensional (2D) as well as three-dimensional (3D) slugs. 2D slugs are good models for slug motility studies [14]. Recently, we found that waves exist in 2D slugs and that slug speed correlates with slug length as found in 3D slugs [15]. Our preliminary observations of substrate deformations indicated that traction force is mainly exerted in the central region of the slug, not in the tip region. In the present work, we detail the main results of the previous short note [15] and compute the forces exerted by the migrating 2D and 3D slugs by using a simplified version of existing methods [10–11]. These experimental data will allow a closer examination of the different models of slug migration [16–19] and illuminate the fundamental role of the sheath in the transmission of forces to the substrate.

2. Materials and Methods

2.1. Cells and culture

Wild-type *Dictyostelium discoideum* NC-4 amoebae were grown according to the standard protocol of two-member culture [20]. Oregon Green 488 (10000 M.W., Molecular Probes) was loaded using electroporation [21]. Recovered cells were mixed at $0.3 \sim 3\%$ with non-loaded cells to prepare slugs.

2.2. DEVELOPMENT OF SLUGS

2D slugs were prepared following Bonner [14] with several modifications. Washed cells were placed on an agar plate (1.5%, Nacalai) in a small drop (2 μL, 10^7cells/mL) together with a drop of mineral oil (Sigma 0.84g/mL, 2 μL) next to it. A cover glass (18 $\times$ 18 mm) was then deposited over them. Plates were incubated for 16 hours at 22 °C. We used 2D slugs that migrated less than a day in all of our measurements. For 3D slugs, 10 μL of a suspension at 10^7 cells/mL was dropped on an agar plate (1.5% agar, Nacalai) and incubated for 16 hours at 22 °C. Development of 2D and 3D slugs on polyacrylamide gel and subsequent substrate deformation experiments were performed in a different experimental room at 21 °C.

2.3. VIDEOMICROSCOPY

Motion of individual cells in 2D slugs were followed by time-lapse epifluorescence using an inverted microscope (Nikon TMD300) equipped with a Xenon lamp (Nikon Xenon, 100W), a standard blue filter set (Nikon FITC), a 20X objective lens, a cooled CCD camera (Princeton Instrument, Pentamax) and a shutter controller (Sutter). Image capturing (typically 0.5 second exposure) and cell center-of-mass tracking were performed with the software Metamorph (Universal Imaging Corp., West Chester, PA). Further analysis of cell shape changes was performed using our own Scion-Image macro (http://www.scioncorp.com). Either the autofluorescence of the cells (2D) or brightfield images (3D) were used to obtain slug velocity data. 2D and 3D slugs on agar were observed at 22 °C.

2.4. ANALYSIS OF CELL MOTION

For each cell analyzed, we stored the time series of the x, y center of mass coordinates, the velocity V, its parallel and perpendicular components with respect to the slug migration direction, the lengths of the major (M) and minor (m) axes of the best fitting ellipse and the angle (θ_M) between the major and the horizontal x-axis. We calculated velocity auto-correlation ρ_{ii} of a given cell i and cross-correlation ρ_{ij} between cells i and j as: $\rho_{ij}(t) = Z_{ij}(t)/Z_{ij}(0)$, where $Z_{ij}(t) = \langle V_i(t_l) \cdot V_j(t_m) \rangle$, $t = |t_l - t_m|$. We used the deformation parameter $D = (M/m) - 1$ to characterize static cell shape. $D = 0$, when the cell shape is a circle. The magnitude of deformation changes was defined as the standard deviation of the deformation parameter. We defined the proportion of polarized cells as the proportion of the histograms $|\theta_S - \theta_M|$ with angles less than 45 °, where θ_S is the slug migration direction as previously done for hydra cells [22].

2.5. POLYACRYLAMIDE GELS

Flexible polyacrylamide gel sheets containing 10% acrylamide, 0.03% bis, ammonium persulfate (APS, 10% w/v solution, 1:133 volume), TEMED (1:1330 volume,

all Bio-Rad products) and 1 μm fluorescent beads (1:50 volume, Molecular Probes) were created and covalently coated with type I collagen (Wako Chemicals, Japan) using Sulfo- SANPAH (Pierce Chemical, Rockford, IL) following published protocols [10, 23]. The Young's modulus of the elastomer was characterized by measuring the deformation of sheets with known weights using the focusing mechanism of the microscope as described in [23]. It was found to be in the range 5–40 kPa in agreement with previously reported results [10].

2.6. Analysis of substrate deformations

Because of the finite depth of field, it is possible to simultaneously record the slug shape with the transmission channel of a confocal microscope (Olympus IX70-KrAr-SPI, Japan) and the small movements of the marker beads with the fluorescence channel (488 nm line). We selected a field of view with the slug approaching on the side and we took the initial image as the undisturbed position to calculate the displacement vector of each bead. The bead centroid position was determined with an accuracy of about 100 nm using our own Scion-Image macros.

2.7. Calculations of forces

In the framework of linear elasticity theory [10], the deformation field *u(r)* inside a semi-infinite elastic medium caused by a distribution of forces *F(r)* on the surface is described by a Fredholm integral equation of the first kind:

$$u_i(r) = \int \mathrm{d}r' G_{ij}(r - r') F_j(r') \tag{1}$$

where i and j refer as the components x, y, z of the vectors and G_{ij} is the Green function, which was calculated in the 19th century by Boussinesq [10, 24]. It was found that the Poisson ratio v of polyacrylamide gels is close to 0.5 [10]. If in addition, one makes the reasonable assumption that there are no perpendicular tractions (i.e., $F_z = 0$), then there is no out of plane displacement. However, the four Green functions Gxx, Gxy, Gyx, and Gyy depend on the bead depth z. We visualized simultaneously the ventral portion of the slugs and the beads located within a shallow depth of the underlying material with 20x or 40x objectives. The inverse problem of calculating forces from displacements, i.e. inverting Equation (1), is a complex computational problem because this kind of Fredholm integral equation is ill posed. The long range spatial extent of the Green function (it scales inversely with distance) smoothes the information [11]. Some studies used, therefore, the raw displacement data themselves as a qualitative map of the local traction [23] sometimes with a local calibration of the displacements in term of forces with a calibrated micropipette [13].

Ill-posed inverse problems can be solved by a regularization method that stabilizes the solution [10, 11, 25]. Recently, it is has been suggested that the inverse problem becomes computationally more efficient when being solved in Fourier space and that regularization is not needed [26]. We use here a simplified method without regularization, which works well for a displacement field averaged in the slug frame on a $Nx \times Ny$ grid divided in rectangular unit cells of about 5–25 μm. At each time, we define a moving slug frame with an origin located on the tip end, and frame axis respectively parallel and perpendicular to slug axis. Slug axis corresponds also to the migration direction as we choose slugs performing mostly a linear steady migration. The grid, the positions and displacements of beads are computed in the moving slug frame. The mean displacement in each unit cell corresponds then to an average of the displacements of different beads over different images.

Forces are calculated on the same grid and divided by the lattice site area to obtain stress components. The integral equation from Equation (1) now becomes a set of linear equations, $u = \mathrm{GF}$, in which $u = (u_x(r_1), u_y(r_1), u_x(r_2), u_y(r_2), \ldots)$, and $F = (F_x(r_1), F_y(r_1), F_x(r_2), F_y(r_2), \ldots)$ are $2N^2$ vectors and G is a $4N^4$ matrix. To solve these equations, we run a numerical program based on iterative biconjugate gradient method [27] generally used to invert large sparse matrix. We impose that the error on the calculated displacements is of the order of the experimental error, i.e., about 0.3 μm due to the depth of field (see the Results Section). Typically, it takes only five iterations for the code to converge to a stable solution. The total grid dimension has little effect on the solution, provided the whole slug is totally located within the grid (i.e., when no forces are exerted outside the grid area). We also checked that the size of unit cell has little effect on the force solution in the range of 15 ± 10 μm.

3. Results

3.1. Individual cell behavior

Approximately 16 hours after starvation, cells have completed aggregation at oil-water interface and 2D slugs of a few cell thick (generally 15–30 μm as measured with the focusing mechanism of the microscope) crawl out from it inside the oil medium (Figure 1a). A sheath appears behind the slugs as it moves forward as found in normal 3D slugs and previous studies of 2D slugs [14, 28]. It is impossible to know if it is a genuine slime sheath or just a band of water between the slug and the oil. In Figure 1a, the sheath has a tubular shape anchored only at some point on the surface as found in case of slugs migrating in the forest soil. Sometimes, however, the sheath is completely collapsed on the surface and flat as found in case of 3D slugs migrating on agar [29]. 2D slugs with sizes ranging between 100 and 460 μm were investigated. Transmission and fluorescence image of a 374 μm long slug are shown in Figures 1b and 1c. The 1% cells loaded with Oregon Green show a good contrast with the autofluorescence of the slug (Figure 1c).

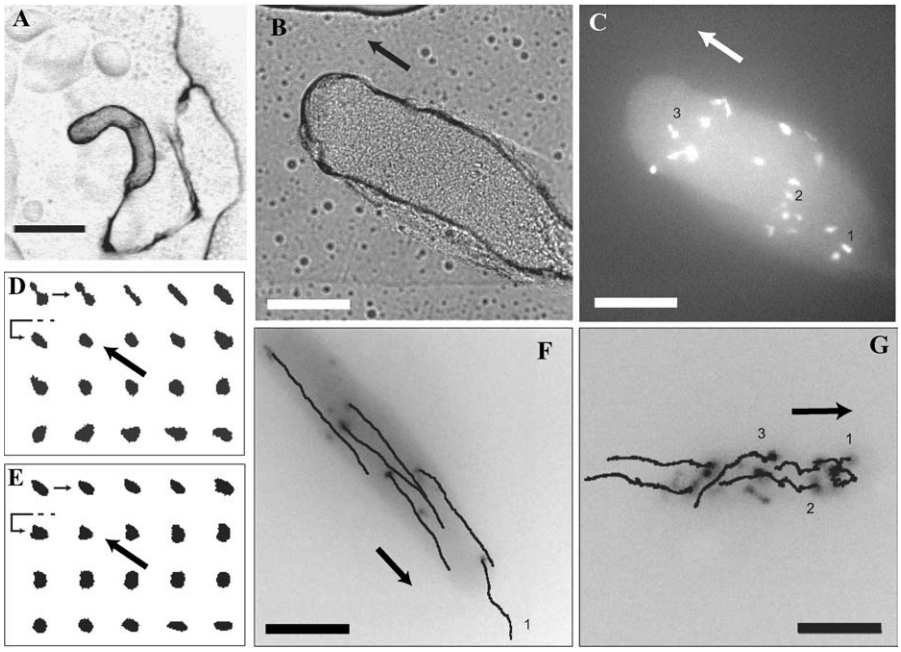

Figure 1. (A) Brightfield image of a 2D *Dictyostelium* slug migrating between an agar surface and mineral oil. Slime sheath trail left behind the slug shows the slug trajectory from the oil/water interface where it formed. Water is on the right hand side. (B) Brightfield image of a 474 μm long slug. (C) The fluorescence image of the same slug shows a few cells loaded with Oregon Green and the autofluorescence from the rest of the slug. (D)–(E) Cell shapes every 1 minute (from left to right) of two cells indexed in (C), respectively the anterior cell 3 (D) and the posterior cell 1 (E). (F) Cell trajectories in a long 2D slug (length: 459 μm). The background image is the inverted fluorescence image showing the cell location at the initial time of the recording. The trajectory of the anterior cell indexed 1 lasts 32 minutes, other trajectories last 36 minutes. (G) Trajectories in a small 2D slug (length: 150 μm) tracked for 25 minutes. The background image corresponds to the final time of recorded trajectories. Posterior cells have a linear trajectory while anterior cell 1 shows a chaotic trajectory. In (B)–(G), thick arrows indicate the slug migration direction. Bars: (A) and (G), 50 μm; others, 100 μm.

It was shown that the anterior cells of 2D slugs correspond mainly to prestalk cells, while posterior cells are mainly prespore cells [28]. Typical cell shapes and trajectories are shown in Figures 1d and g. Anterior cells (i.e., cell 3 in Figure 1c) behave as isolated amoebae, they seem to advance by pushing out pseudopodia and lamellipodia and then pulling out their rears (Figure 1d). They move often laterally in a more or less chaotic way, which is more pronounced for small slugs. In Figure 1g for instance, cell 1 makes a loop. In long slugs (Figure 1f), the fast overall migration of the slug makes the lateral displacements of anterior cells less obvious. Posterior cells (i.e., cells 1 and 2 in Figure 1c) also show alternatively elongated and rounded shapes, but to a lesser extent both in terms of amplitude and frequency (Figure 1e). They always move straight in the direction of slug

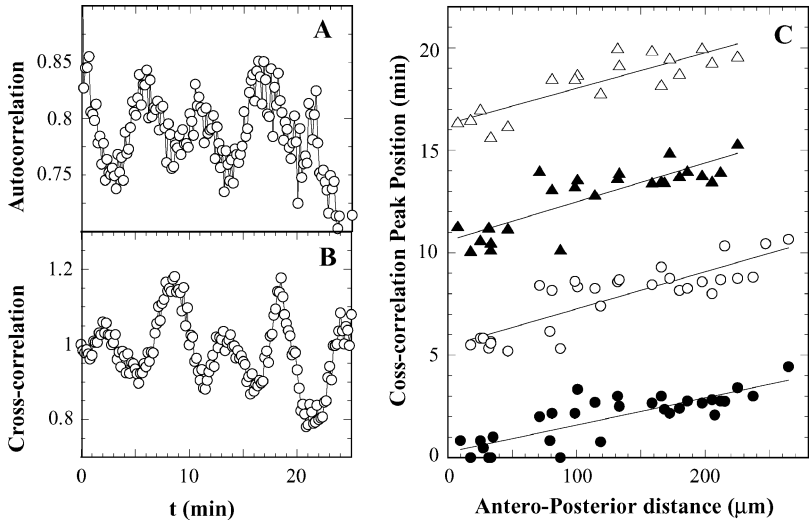

Figure 2. (A) Velocity auto-correlation of the posterior cell 1 of Figure 1C. (B) Velocity cross-correlation of cells 1 and 2 of Figure 1C. (C) Position of the cross-correlation peaks as a function of the antero-posterior distance between cells of Figure 1C. Bullets to open triangle correspond respectively to the first to fourth peak of correlation. Solid lines are linear fits.

movement. Both the mean velocity and the standard deviation of the velocity are larger for anterior cells than for prespore cells. Posterior cells, though they present some periodic movements (see below), move roughly at slug velocity. For instance, for the slug of Figure 1g moving at 2.7 μm/minute, we measured $V = 3.1 \pm 1.9$ as an average over three prepore cells and $V = 4.4 \pm 4.0$ for four anterior cells (mean $\pm$ standard deviation in μm/minute). Although it is sometimes subjective, we have distinguished in the following these two groups of cells.

Figure 2a shows the velocity auto-correlation function in a long 2D slug (cell indexed 1 in the slug of Figure 1c). Velocity oscillates with a period of 5.5 minutes with a peak–peak amplitude, which is only 12% of the total velocity magnitude. We investigated the movements of fluorescent labeled cells in 30 slugs. In 13 slugs, we found periodicity (mostly but not only posterior cells). Cell velocity is also correlated spatially with other cells as Figure 2b shows clearly five oscillations in the cross-correlation of the velocity of the two cells indexed 1 and 2 in Figure 1c. The peaks in the cross-correlation represent the phase differences between the velocity oscillations of the two cells. We analyzed the relation between the phase of the oscillations and the cell coordinates as previously done by Breen and Williams for 3D slugs [4]. In Figure 2c, we have plotted the positions of the first four peaks as a function of the cell–cell distance along the slug's antero-posterior axis. The position of each peak increases linearly with the antero-posterior distance. They share the same slope and are shifted by the same period, i.e., 5.5 minutes, which agrees well with the period obtained from cell velocity autocorrelation data. Hence,

these data unambiguously indicate that traveling waves of movement are present in 2D slugs. The speed of wave propagation is given by the slope of the curves of Figure 2c, i.e., 55 μm/minutes for this slug.

3.2. Dependence of slug speed and individual cell behavior on slug length

We measured as a function of slug length the speed of 2D and 3D slugs. Despite the presence of mineral oil and the cover-glass on top, the 2D slug speed increases with its length, and it overlaps with 3D speed (Figure 3). Our 3D measurements (filled circles) are in good agreement with those reported by Inouye and Takeuchi (squares) [30]. The dependence of slug speed on slug length is not linear. We also reported on Figure 3 the speed of slugs migrating on the polyacrylamide substrate used for force measurements. There are very similar to those found on agar. Small difference may be due to a slightly colder temperature (21 °C instead of 22 °C) in the experimental room were we carried out these experiments on polyacrylamide substrate.

We studied as a function of slug length the average parallel and perpendicular components of cell velocity (Figures 4a and b), cell shape changes (Figure 4c) and the proportion of polarized cells (Figure 4d) for each cell type. The average is taken over the whole cells and the whole times analyzed in a given slug. There are no clear differences between the parallel component (i.e., in the direction of

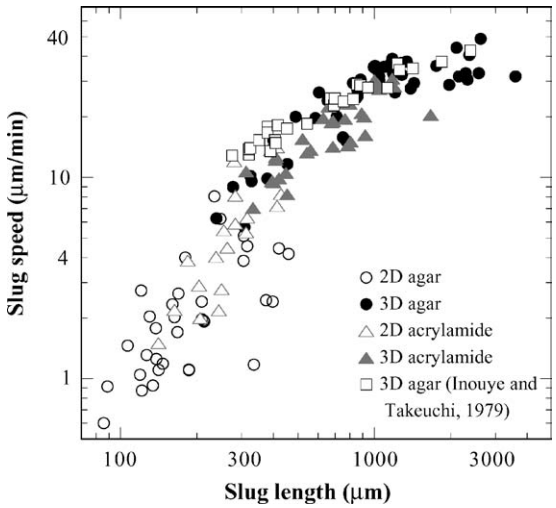

Figure 3. Slug speed as a function of slug length. Open and filled circles correspond respectively to 2D and 3D slugs on agar. Open and filled triangles correspond to 2D and 3D slugs on polyacrylamide substrates. Squares correspond to the measurements of Inouye and Takeuchi [30] for 3D slugs on agar. Note that the value of the 3D velocities on agar previously reported [15] was wrong by a constant factor of about 0.6.

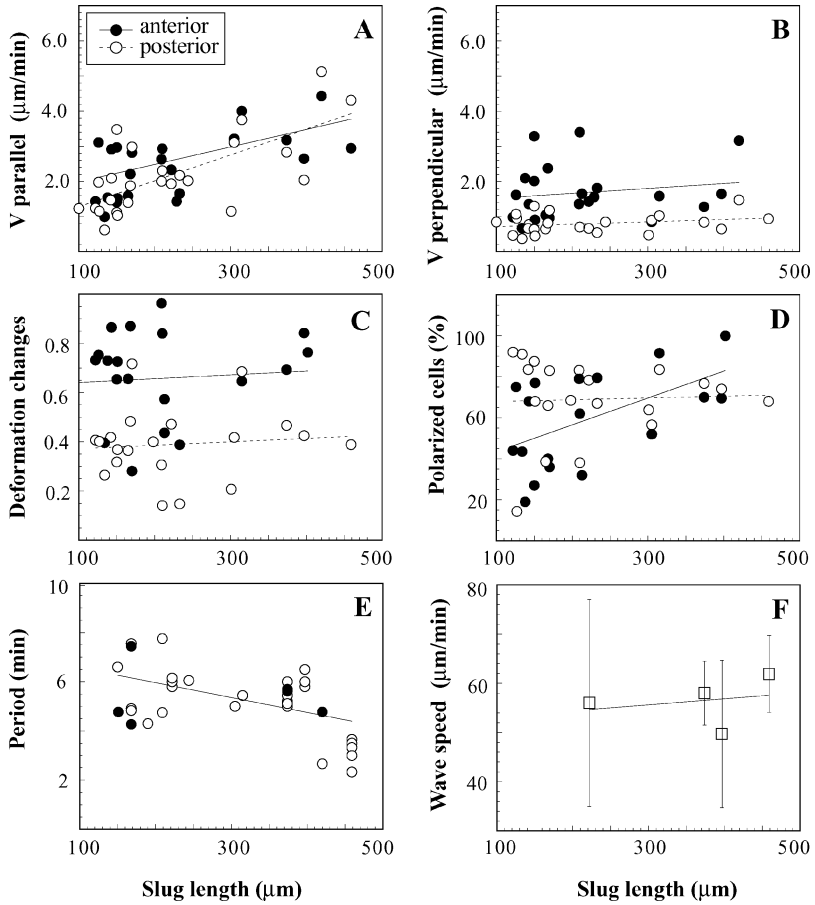

Figure 4. Relationship between slug length and individual cell motion components for anterior (bullets) and posterior cells (open circles) except (F) where the wave speed is calculated using the whole cell data. Solid and dotted lines represent linear fit of respectively anterior and posterior cells. (A) Parallel and (B) Perpendicular component of cell velocity with respect to the direction of slug migration. (C) Magnitude of cell deformation changes.(D) Proportion of polarized cells defined as the proportion of the histogram $|\theta_S - \theta_M|$ with angles less than 45. (E) Period of velocity oscillations calculated from the auto-correlation curves of individual cells. (F) Speed of wave propagation in 2D slug calculated from the cross-correlation analysis.

slug migration) of both anterior and posterior cells. It is increasing with slug length and roughly equal to slug speed (Figure 4a). On the other hand, the perpendicular velocity component is approximately twice larger for anterior cells (Figure 4b). This quantity is weakly dependent on slug size. The magnitude of cell shape changes (standard deviation of the deformation parameter) is 1.5 larger for anterior cells than for posterior cells (Figure 4c). This quantity is weakly dependent on slug length. In small slugs, the proportion of polarized cells (see material and methods) is less than 50% for anterior cells (Figure 4d). It indicates that anterior cells in small slugs

deform (and move) mainly in a direction orthogonal to the slug direction. However, the proportion of polarized anterior cells increases with slug length. On the other hand, posterior cells are highly polarized in the direction of slug migration.

The period of velocity oscillation ranges between 2.3 and 7.7 minutes for the 41 cells (belonging to 13 slugs) presenting oscillations in their autocorrelation (Figure 4e). The period depends little on cell type and apparently decreases slightly with slug length. In average, we find a period of 5.2 $\pm$ 1.2 minutes (mean $\pm$ standard). Periodic movements exist only in the longer slugs investigated (larger than 150 μm). The percentage of slugs with correlated cells is 58% (7:12) in slugs with a length between 150 and 300 μm and 86% (6:7) in slugs larger than 300 μm. Wave analysis is more difficult to achieve, because only long slugs with a large number of fluorescent cells allow wave detection. We detected waves in four slugs, the smaller is 222 μm long. Wave speed seems to be independent on the 2D-slug length (Figure 4f). The average wave speed is 56 $\pm$ 10 minutes.

3.3. Substrate deformations and traction forces during slug migration

Shape of *Dictyostelium* amoebae on polyacrylamide substrates treated with type I collagen appear indistinguishable from those cultured on agar. Cells spread well and are able to aggregate. The resulting 2D slugs migrate at the same speed than slugs of the same length on agar (Figure 3). Both slugs and isolated cells (not shown) induce displacements of fluorescent beads.

Figure 5a shows the transmission image (at $t = 15$ minutes) of an elongated 2D slug (280 μm long, 70 μm wide and 20–30 μm thick as measured with the microscope). The slug is moving in the oil medium from left to right in a rectilinear fashion ($v = 12$ μm/minutes) with a tubular slime sheath left behind. Initially, it was at the extreme left boundary of the recorded field of view. Figures 5b and 5c show the displacement field of this slug at two different times (i.e., $t = 10$ and 15 minutes). Each arrow starts at the position of a bead centroid at $t = 0$, which is assumed to be in the undisturbed state. Ahead from the slug tip on the right (Figure 5b), deformations are indeed weak, spatially uniform and directionally isotropic. Unlike the slug speed and the slug direction which are almost constant, substrate deformations show at every time a characteristic pattern in the slug frame. Deformations are absent in the tip region. In the central region, they present a parallel component from a direction opposite to slug migration and a perpendicular component directed centrifugally (Figures 5b and 5c). Far behind the slug, the beads almost returned to their initial position (not shown).

The deformation field has been averaged in the moving slug frame in Figure 5d using a 32 $\times$ 32 grid with spacing of 12.6 and 4.8 μm along slug axis and perpendicular direction, respectively. We used this averaged data set to compute the force field of Figure 5e. This force field presents slightly erratic vectors in its lower part. This is due to the fact the displacement field in this lower part is not as regular as in

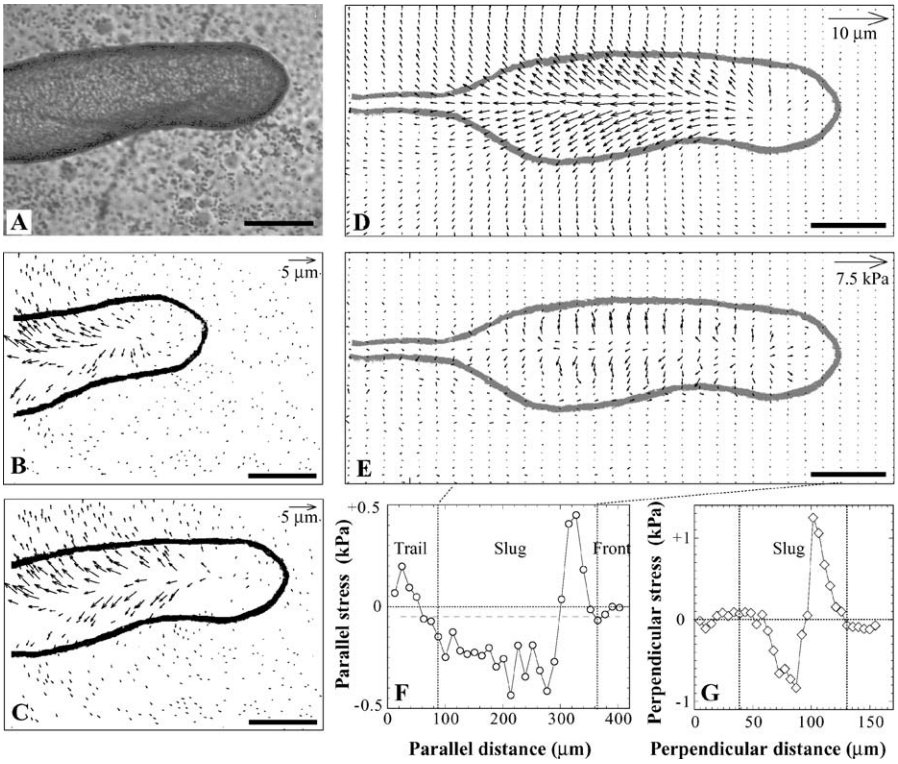

Figure 5. Bead displacement and force vector field of an elongated 2D slug ($L = 280$ μm) moving on polyacrylamide elastomer (Young modulus, $E = 5$ kPa) from left to right at v = 12 μm/minutes. (A) Transmission image of the slug at $t = 15$ minutes. (B–C) Bead displacement vector field calculated between initial time 0 and $t = 10$ minutes (B), $t = 15$ minutes (C). (D) Bead displacement vector field averaged in the moving slug frame. General slug shape is represented. (E) Force field calculated from the averaged deformation field with a bead depth $Z = -5$ μm. Scale of bead displacements and stresses (force per unit area) are given in (D–E). All scale bars, 50 μm. (F) Parallel component of the force field averaged over six central rows as a function of distance along slug axis. Dashed line is the mean parallel stress (i.e., -50 Pa). (G) Perpendicular component of the force field averaged over 19 central columns as a function of distance perpendicular to slug axis.

the upper part. We believe that irregularities are due to beads at different depths in the elastomer. For a same force exerted at the surface, beads at different depth will indeed present different displacements. Here, regularization methods [10–11] will probably smooth the computed force field. We have calculated the bead displacement vector field predicted from the force field of Figure 5e by back-substitution into Equation (1) (see Materials and Methods). To the eye, no difference is visible from the experimental field of Figure 5d (not shown). This solution was obtained in six iterations and the mean vector error $|\mathrm{GF} - u_{\mathrm{exp}}|$ is 0.28 μm. This value is larger than the estimated resolution for the bead center of mass (i.e., 0.1 μm). The error is in fact due to the uncertainty in the relative bead depth which affect the

Green functions. Changing the absolute mean bead depth (i.e., using $Z = -2.5$ or $Z = -7.5$ instead of $Z = -5$ μm) in the calculations also has an important effect, at least quantitatively, on the resulting force field. The control of the microscope focusing plane seems then the most important point to obtain reliable quantitative estimates of forces. On the other hand, we checked that adding Gaussian noise with standard deviation 0.1 μm to the experimental displacement field only changes by 25% the magnitude of the average forces calculated, but not the qualitative pattern. This relative change is similar to what was found using a regularization method [11] and may be used as an estimate of the noise in the calculated forces.

We describe now the overall characteristics of the force field. We have computed for that the average parallel and perpendicular force per unit area (stress) components as a function of parallel and perpendicular distances (Figures 5f and g). Parallel direction is the direction of slug migration. The average is taken over the six central rows and the 19 central columns of the slug respectively. As expected from the deformation field, forces are almost absent in about the first 20 μm along the slug axis from the tip. Just after this force free area, one finds positive stress at 0.45 kPa indicating a resistive force here. Surprisingly, in the central part of the slug, the largest forces are mainly directed perpendicularly to the slug axis, roughly symmetric with respect to this axis, with a maximum perpendicular stress around 1 kPa (Figure 5g). In about a 15 μm wide layer on the periphery, but still inside the slug, forces vanish (Figure 5g). The parallel component in the central part of the slug is negative (-0.3 ± 0.1 kPa), indicating dominance of traction here (Figure 5f). Note that forces are almost absent outside the slug boundaries (Figure 5e) without constraining the solution for that purpose [10–11]. There are not very well defined in the tail, but generally seem weakly resistive (Figure 5f). The overall mean parallel force is -0.05 kPa not significantly different from zero. As expected for a slowly locomoting body, viscous forces with the external medium can be neglected, moreover, acceleration can be also neglected as the slug is moving at nearly constant speed. As a result, there is no net force transmitted to the substrate [25, 26].

We have recorded the substrate deformations caused by several 2D slugs. The force pattern seems to depend greatly on the slug thickness, though we could not obtain unambiguous force solutions for each (either because the bead distribution was too sparse, or because we obtained also forces outside the slug area, mainly in the tail). In some thick 2D slugs, the displacement (and probably force) free area in the anterior slug part may extend up to 150 μm from the tip (not shown). In the later case, the tip seems constantly raised in the air, a close contact with the substrate (and probably traction forces) exists mainly in the posterior region. Once, we recorded a very thin slug, without visible sheath, almost flat and purely 2D as found previously by Bonner [14]. The displacement pattern presents an interesting loop on the sides (Figures 6b and 6d) similar to the dipolar electric field. This is the deformation field expected from a point-like horizontal force monopole, oriented backward [11]. The reentrant part of the loop is generally hardly visible as in

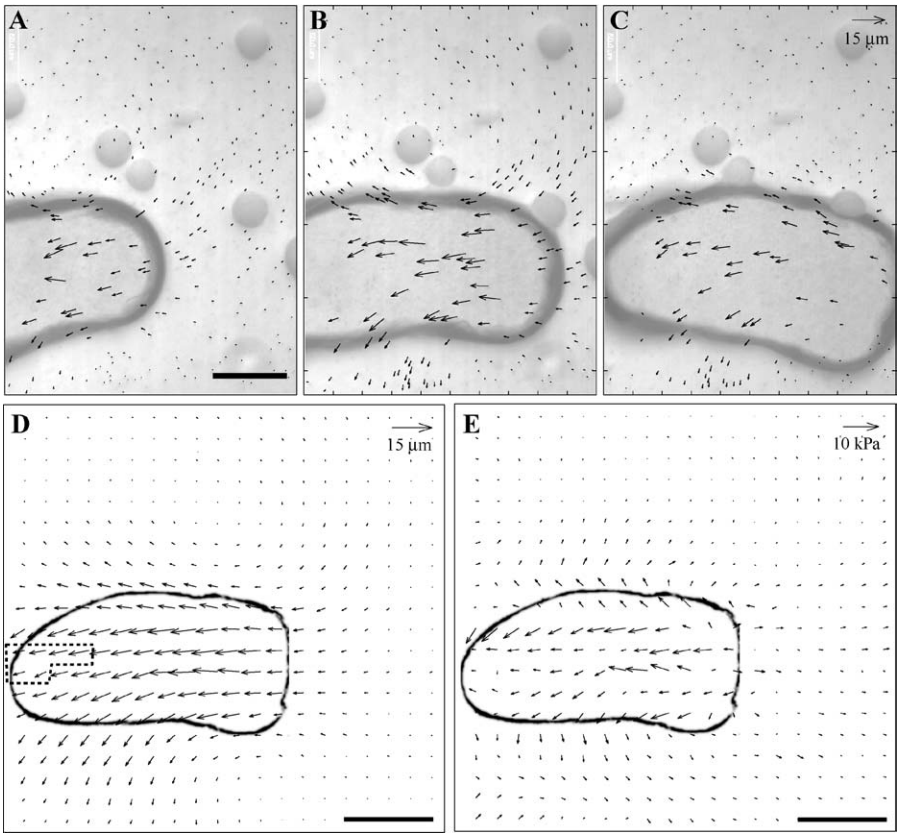

Figure 6. Bead displacement and force vector field created by a small flat 2D slug ($L = 158$ μm) moving on polyacrylamide elastomer (Young modulus, E = 25 kPa) from left to right at $v = 2.7$ μm/minute. (A–C) Bead displacement vector field calculated between initial time 0 and $t = 20, 40$ and 60 minutes. (D) Bead displacement vector field averaged in the moving slug frame. General slug shape is represented. Vectors surrounded by a dotted line were interpolated from neighbors. (E) Force field calculated from the averaged deformation field with a bead depth $Z = -7.5$ μm. Scale of bead displacements and stresses (force per unit area) are given in (D–E). All scale bars, 50 μm.

Figures 5b and d and 7a and b. It indicates that the relative magnitude of friction in the tip and perpendicular forces are less important with respect to the traction forces in the flat 2D slug. The force field calculated is noisy, due to sparse bead distribution in particular in the posterior region of the slug (unit cells surrounded by a dotted line where interpolated in Figure 6d), and forces do not perfectly vanish outside the slug, however, the force field shows qualitatively these features: weak friction and weak perpendicular forces (Figure 6e). Contrary to Figures 5e and 5g, it is clear that there is a net negative traction force not balanced. We believe that the missing force comes from the glass covering the 2D slugs. Even if *Dictyostelium* amoeba poorly spread on glass, ruling out to our opinion the possibility that the

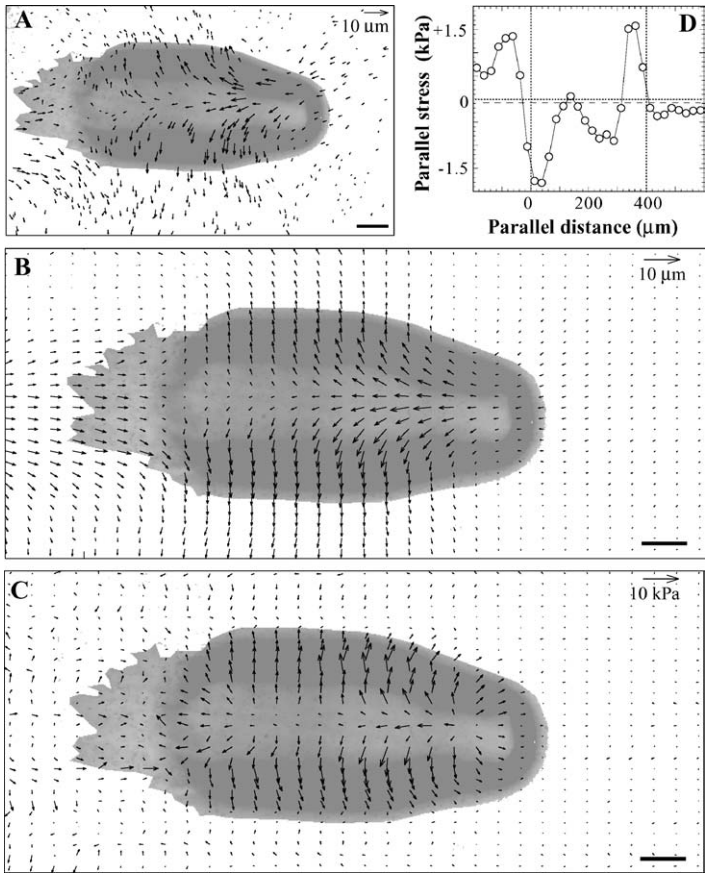

Figure 7. Bead displacement and force vector field of a 3D slug ($L = 400$ μm) moving from extreme left of the recorded field ($t = 0$) to right in a rectilinear fashion ($v = 9.75$ μm/minute) on polyacrylamide elastomer (Young modulus, $E = 25$ kPa). (A) General slug shape together with the rear of the slime sheath and bead displacement vector field at $t = 40$ minutes. (B) Bead displacement vector field averaged in the moving slug frame. (C) Force field calculated from the averaged deformation field with a bead depth $Z = -21$ μm. (D) Parallel component of the force field averaged over six central rows as a function of distance along slug axis. Dashed line is the mean parallel stress (i.e., -85 Pa). All scale bars, 50 μm.

cell mass gets traction from the rigid glass, it is possible that resistive forces are transmitted to the glass (direct slug/glass friction, or due to protrusive defects in elastomer or to water droplets in oil as those visible in Figures 6a and c).

In order to validate the experimental methods, the force calculations and the qualitative features of force field found for 2D slugs, we have performed force experiments on a freely migrating 3D slug in air on a polyacrylamide substrate (without oil and cover glass).

The 3D slug of Figure 7a is 400 μm long, 190 μm wide. It is moving from left to right at $V = 9.75$ μm/minute. A large collapsed slime sheath (as much as

large as the slug width) was left behind the slug during its migration. We have represented its more visible rear end part in the background of Figure 7a together with slug outline. It resembles the sheath usually found for 3D slugs on agar. The bead displacements (Figure 7a at $t = 40$ minutes or Figure 7b for the averaged data in the slug frame) present a novel characteristic compared to the 2D slug analyzed. The tail region presents large positive bead deformations (Figure 7b). On the slug sides, we find large perpendicular deformations directed toward the periphery of the slug. The force field obtained from the averaged deformations (Figure 7b) is shown in Figure 7c. The mean vector error $|\mathrm{GF} - u_{\mathrm{exp}}|$ is 0.3 μm close to the value found for the 2D slug (Figures 5d and 5f). Forces are very symmetric with respect to slug axis. They are present in the slug area and vanish at the slug boundary except on the tail area (see below).

Again we find a large perpendicular component of the force directed toward the periphery on the sides of the slug. The magnitude of these perpendicular forces increases from the slug axis to a maximum of about 4.1 kPa at mid distance from the periphery and then slightly decreases. Forces are in fact almost perpendicular to the slug boundary on the periphery. Figure 7d shows mean parallel component profile as a function of distance along slug axis. Forces, null at the tip end and outside, increase quickly to $+0.9$ kPa between 50 and 75 μm from the tip (resistive forces). Traction becomes larger than friction only at about 100 μm from the tip with a first minimum at -0.9 kPa (at 140 μm from the tip). Parallel forces almost vanish in the central part of the slug (at 260 μm from the tip) and decrease again in the very posterior part of the slug to -1.8 kPa. Behind the slug area, in the area occupied by the trail of the slime sheath forces are clearly positive though the data are noisy. This is due to poor statistics in computing the averaged bead deformation field in this region (Figure 7b). We can evaluate however a mean resistive force of $+1.0 \pm 0.5$ kPa corresponding probably to the resistive force transmitted by the collapsed sheath to the substrate. The overall force balance is respected as the mean parallel net force is only -0.085 kPa (dashed line in Figure 7d).

4. Discussion

4.1. Results obtained with 2D slugs may apply directly to normal 3D slugs

Bonner [14, 28] noted that 2D slugs share most of their properties with 3D slugs. From our extensive analysis of cell motion within 2D slugs, we are able to extend the set of shared properties between 2D and 3D slugs. (i) The velocity of 2D slugs is proportional to slug length and length-velocity plots of 2D slugs overlap with those of 3D slugs in spite of differences in surrounding condition such as mineral oil and coverglass. (ii) Most of the cells present at least regular oscillations of their velocity. Waves of movement exist in the longer 2D slugs analyzed. Our estimates of average wave speed and periodicity (i.e., 56 ± 10 μm/minute and 5.2 ± 1.2 minutes, respectively) are similar to previous measurements in 3D slugs using

various methods [4, 6, 31], (iii) We occasionally observed spiral motion in a plane perpendicular to slug migration at the tip of a large 2D slug (not shown). This slug was certainly thicker than the others as we sometimes lost partially focus during the cell rotation. Thus, it seems likely that there is a continuous cross-over in between 2D and 3D slugs using our method of preparation.

4.2. Role of chemoattractant waves and slug length dependence of the slug speed

The fact that wave speed is weakly dependent on 2D slug length and similar to measurements in 3D slugs, suggests this quantity depends mainly on the wave detection and relay properties of the cell, not on the slug geometry. On the other hand, the apparent slight decrease of the period of velocity with slug length was never reported (Figure 4e). The perpendicular component of the velocity (Figure 4b) and the amplitude of deformations changes (Figure 4c) are larger for anterior than posterior cells, but also weakly dependent on slug length. The proportion of polarized anterior cells seems to increase with slug length (Figure 4d). The chemoattractant waves may play this role, which is to polarize the cell deformations in the migrating direction. Another possible role of chemotaxis is to increase the motive force of the cells. Of course, a main issue of our future force measurements is to find whether waves of forces exist. For the moment let us just comment that many recent models of slug proposed that cells exert forces only when they experience a positive gradient of chemoattractant. As a result, slug speed increases with slug length but saturates when it exceed the wavelength migration [18, 19]. In these models, slugs larger than the wavelength were not investigated. Figure 3 clearly shows that slug speed still increases by a factor of 8–10 between the wavelength (250 μm) and the larger 3D slugs observed (3 mm). Something important is then not captured by models. The hypothesis that the motive force of the slug is proportional to its volume and not to the contact surface with the substratum for instance, initially deduced from experiments by Inouye and Takeuchi [7, 30], merits a closer examination as it is the hypothesis generally assumed to model slug migration [16–19]. An other possible candidate is that the friction forces are more complicated than a simple viscous drag proportional to the slug velocity [16–18, 30].

4.3. Distribution of forces in migrating slugs, role of slime sheath

Perhaps the more intriguing result of this paper is the existence of large forces perpendicular to the direction of slug migration, symmetric with respect to this axis (4.1 kPa in Figure 7c). This is clearly visible in the 3D slug of Figure 7c as well as in the relatively thick 2D slug of Figures 5e and f. On the other hand, forces are mainly parallel to slug axis in thinner 2D slugs (Figure 6). Although we did not follow cell movements in the force assay experiments, we never observed

significant lateral movements in 2D slugs, especially in the central prespore part of the slug. Symmetric lateral movements from the slug axis toward periphery have never been reported to our knowledge in case of 3D slugs. Moreover, cells present sometimes alternatively elongated shapes but mostly in the slug direction (Figure 4d). Therefore, the observed perpendicular forces do not correspond to traction nor friction resulting from the lateral movements of the cells. We believe they result from the mechanical forces transmitted by the slime sheath to the substrate.

The slime sheath is a glycoprotein surface coat synthesized by the cells, completely surrounding the slug. As the slug advances, new surface sheath is continuously formed and it is left behind as a collapsed tube [29]. Once the sheath makes contact with the substrate it attaches strongly to it and acts as a protective shell for the slug. It seems likely that newly formed sheath in the anterior part of the slug can be deformed by anterior cells, but posterior part is more rigid [32]. We postulate that (i) this elastic sheath shell is continuously maintained under tension by the cell mass, (ii) the slug as a whole has an ellipsoidal shape truncated on the contact area with the surface (Figure 8), (iii) sheath is firmly anchored in different points in the contact area. Then, due to its tension, the sheath can pull out the elastic substrate in the direction tangential to the slug profile, where it is anchored, i.e., mostly around the contact line between slug, external medium (oil or air) and substrate. These stretching forces are referred as $\boldsymbol{S}$, $\boldsymbol{S}'$ or $\boldsymbol{S}''$ in Figure 8. Of course, the sheath is not an ideal surface, it is made of protein filaments attached at different points in the vicinity of the contact line. Perpendicular forces are then also distributed underneath the slug.

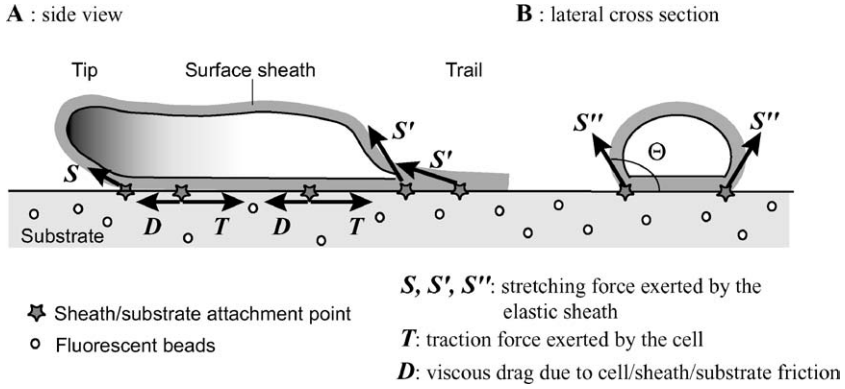

Figure 8. Proposed forces acting on a *Dictyostelium* slug migrating on a planar surface. The slug is surrounded by a viscoelastic sheath which is attached to the substrate in many points in the contact area. Forces generated by the moving cell mass are transmitted to the substrate by the sheath at these attachments points. Forces in the contact area are the traction $\boldsymbol{T}$ exerted by the cells and the viscous drag $\boldsymbol{D}$ due to the cell/sheath/substrate friction. In the contact line surrounding the contact area, the stretched sheath pulls out the elastomer in a direction tangent to slug profile ($\boldsymbol{S}$, $\boldsymbol{S}'$, $\boldsymbol{S}''$).

As the elastic substrate assays do not visualize vertical bead displacements, we visualize only the in-plane component of the stretching forces, which is perpendicular to the projection of slug boundary. In case of 3D or thick 2D slugs with a contact angle Θ larger than 90° (Figure 8b), the in-plane force is directed outward (Figures 5e and 7c). In case of pure 2D slugs, perpendicular forces are not important possibly because sheath tension is small. Our hypothesis that the sheath transmits forces to the substrate in the vicinity of contact lines also explain the resistive forces in the tip and in the tail region (Figure 7c) as the corresponding tangent directions are both directed forward for a thick 2D slug or a 3D one (Figure 8a).

4.4. Order of magnitude of traction and friction forces

The question of where lies the motive force for slug movement is an old and contentious issue (as reviewed in [15]). We believe our force measurements answer definitely to this question. We find generally that forces (at least traction forces) are absent in the front of the tip region of 3D and most 2D slugs (except the flat slug of Figure 6). It is unlikely that traction and resistive forces (see below) compensate exactly each other. We believe the absence of force is rather due to the vertical raising of the tip may as found in 3D slugs [4, 5]. The fact that forces exist in the tip of flat 2D slugs (Figure 6) supports also this conclusion. Therefore, forces are exerted when a physical contact exists with the substrate. For that reason, the absence of force in the central region of the 3D slug of Figures 7c and 7d is probably due to the presence of an arch in this region as already found for old 3D migrating slugs viewed from the side [5].

Resistive forces $\boldsymbol{R}$ in the tip and trail region result probably from the previously described force due to sheath tension but also to a viscous drag due to cell/substrate friction or cell/sheath friction transmitted to the substrate ($\boldsymbol{S}$, $\boldsymbol{S}'$ and $\boldsymbol{D}$, respectively in Figure 8a). By assuming tractions are absent in this region, we find an estimate of $\boldsymbol{R} = +0.45$ and $+0.9$ kPa for the tip resistive force of slugs of Figures 5 and 7, respectively. In the central part of the slug of Figure 5e, by assuming that the same resistive force exists than in the tip (at least the order of magnitude should be correct), we can evaluate the traction force per unit area $\boldsymbol{T}$ from the resulting negative parallel force ($\boldsymbol{T} + \boldsymbol{R} = -0.3$ and -0.9 kPa, respectively). We find $\boldsymbol{T} = -0.75$ and -2.7 kPa for the thick 2D and the 3D slug, respectively. These preliminary orders of magnitude are in agreement with the measurements of Inouye and Takeuchi [7] who found that the motive force of 3D slugs inside agar capillaries is proportional to its volume, the value per unit volume being 58 pN/μm^3. Indeed, if we divide our forces per unit area by the slug thickness (about 25 μm and 100 μm, respectively), then we find approximately 30 pN/μm^3. We are currently working to improve the resolution (both spatial and in force) by increasing bead concentration and improving their detection. We are also trying to improve the elastomer calibration and the bead depth estimation to improve the reliability on the absolute force measurements.

5. Conclusions

We have studied extensively the movements including deformations of fluorescent cells in thick 2D slugs. Basically, we found the same features as in 3D slugs [5]. We then performed the first measurements of the distribution of forces in migrating *Dictyostelium* slugs. The distribution of forces transmitted to the substrate appears much more complex than usually assumed in models. We find successive regions of friction (tip and tail) and traction (central part) oriented in the slug axis as well as large perpendicular forces. We make the hypothesis that the latter is due to the elastic forces exerted by the stretched sheath. It is then challenging to understand how this complex force pattern may generate a well defined length-dependence of slug velocity.

Acknowledgements

J.P.R. acknowledges support from the Japan Society for the Promotion of Science (Invitation Fellowship for Research in Japan, Long Term, FY2002, FY2003). The warm hospitality of Pr. S. Iwasaki at Tohoku Institute of Technology is acknowledged. Part of this work was done in Photodynamics Research Center (PRC). We acknowledge Prof. J. Nishizawa and Prof. S. Ushioda for usage of the optical facilities at PRC. We would like also to thank Anne Tanguy and Daniel Riveline for useful discussions.

References

[1] Dormann, D., Siegert, F. and Weijer, C.J.: Becoming Multicellular by Aggregation; The Morphogenesis of the Social Amoebae Dicyostelium Discoideum, *J. Biol. Phys.* **28** (2002), 765–780.

[2] Maeda, Y.:Role of Cyclic AMP in the Polarized Movement of the Migrating Pseudoplasmodium of *Dictyostelium discoideum*, *Dev. Growth Differ.* **19**(1977), 201–205.

[3] Siegert, F. and Weijer, C.J.: Three-Dimensional Scroll Waves Organize *Dictyostelium* Slugs, *Proc. Natl. Acad. Sci. USA*. **89**(1992), 6433–6437.

[4] Breen, E.J. and Williams, K.L.: Optical Flow Analysis of the Ventral Cellular Layer of the Migrating *Dictyostelium discoideum* Slug, *Microbiology* **140**(1994), 1241–1252.

[5] Dormann, D., Siegert, F. and Weijer, C.J.: Analysis of Cell Movement During the Culmination Phase of *Dictyostelium* Development, *Development* **122**(1996), 761–769.

[6] Dormann, D. and Weijer, C.J.: Propagating Chemoattractant Waves Coordinate Cell Movement in *Dictyostelium* Slugs, *Development* **128**(2001), 4535–4543.

[7] Inouye, K. and Takeuchi, I.: Motive Force of the Migrating Pseudoplasmodium of the Cellular Slime Mould *Dictyostelium discoideum*. *J. Cell Sci.* **41**(1980), 53–64; Inouye, K.: Measurement of the Motive Force of the Migrating Slug of *Dictyostelium Discoideum* by a Centrifuge Method, *Protoplasma* **121**(1984), 171–177.

[8] Eliott, S., Vardy, P.H. and Williams, K.L.: The Distribution of Myosin II in *Dictyostelium Discoideum* Slug Cells, *J. Cell Biol*. **115**(1991), 1267–1274.

[9] Early, A., Abe, T. and Williams, K.L.: Evidence for Positional Differentiation of Prestalk Cells and for a Morphogenetic Gradient in *Dictyostelium*, *Cell* **83**(1995), 91–99.

[10] Dembo, M. and Wang, Y.-L.: Stresses at the Cell-to-Substrate Interface During Locomotion of Fibroblasts, *Biophys. J.* **76**(1999), 2307–2316.

[11] Schwarz, U.S., Balaban, N.Q., Riveline, D., Bershadsky, A., Geiger, B. and Safran, S. A.: Calculation of Forces at Focal Adhesions from Elastic Substrate Data: The Effect of Localized Force and the Need for Regularization, *Biophys. J.* **205**(2002), 2583–2590.
[12] Beningo, K.A. and Wang,Y.–L.: Flexible Substrata for the Detection of Cellular Traction Forces, *Trends Cell Bio.* **12**(2002), 72–84.
[13] Uchida, K.S., Kitanishi-Yumura, T. and Yumura, S.: Myosin II Contributes to the Posterior Contraction and the Anterior Extension During the Retraction Phase in Migrating *Dictyostelium* Cells, *J. Cell Sci.* **116**(2003), 51–60.
[14] Bonner, J.T.: A Way of Following Individual Cells in the Migrating Slugs of *Dictyostelium Discoideum*, *Proc. Natl. Acad. Sci. USA*. **95**(1998), 9355–9359.
[15] Rieu, J.-P., Tsuchiya, K., Sawai, S., Maeda, Y. and Sawada. Y.: Cell Movements and Traction Forces on Elastic Substrates During the Migration of 2-Dimensional *Dictyostelium* Slugs, *J. Biol. Phys.* **29**(2003), SN1–SN4.
[16] Umeda, T. and Inouye, K.: Theoretical Model for Morphgenesis and Cell Sorting in *Dictyostelium Discoideum*, *Physica D.* **126**(1999), 189–200.
[17] Palsson, E. and Othmer, H.G.: A Model for Individual and Collective Cell Movement in *Dictyostelium Discoideum*, *Proc. Natl. Acad. Sci. USA*. **97**(2000), 10448–10453.
[18] Vasiev, B. and Weijer, C.J.: Modelling of *Dictyostelium Discoideum* Slug migration, *J. Theor. Biol.* **223**(2002), 347–59.
[19] Marée, A.F., Panfilov, A.V. and Hogeweg, P.: Migration and Thermotaxis of Dictyostelium Discoideum Slugs: A Model Study, *J Theor Biol.* **199**(1999), 297–309.
[20] Bonner, J.T.: Evidence for the Formation of Cell Aggregates by Chemotaxis in the Development of the Slime Mold *Dictyostelium Discoideum*, *J. Exp. Zool.* **106**(1947), 1–26.
[21] Sawai, S., Hirano, T., Maeda, Y. and Sawada, Y.: Rapid Patterning and Zonal Differentiation in a Two-Dimensional *Dictyostelium* Cell Mass: The Role of pH and Ammonia, *J. Exp. Biol.* **205**(2002), 2583–2590.
[22] Rieu, J.-P., Upadhyaya, A., Glazier, J.A., Ouchi, N.B. and Sawada, Y.: Diffusion and Deformations of Single *Hydra* Cells in Cellular Aggregates, *Biophys. J.* **79**(2000), 1903–1914.
[23] Pelham, R.J. and Wang, Y-L.: High Resolution Detection of Mechanical Forces Exerted by Locomoting Fibroblasts on the Substrate, *Mol. Biol. Cell.* **10**(1999), 935—945.
[24] Landau, L.D. and Lifshitz, E.M.: *Theory of Elasticity*, (3rd edn.), J.B. Sykes and W.H. Reid (translators), Pergamon Press, Oxford, UK, 1986.
[25] Dembo, M., Oliver, T., Ishihara, A. and Jacobson, K.: Imaging the Traction Stresses Exerted by Locomoting Cells with the Elastic Substratum Method, *Biophys J.* **4**(1996), 2008–2022.
[26] Butler, J.P., Tolic-Norrelykke, I.M., Fabry, B. and Fredberg, J.J.:Traction Fields, Moments, and Strain Energy that Cells Exert on their Surroundings, *Am. J. Physiol. Cell Physiol.* **282**(2002), C595–C605.
[27] Press, W.H., Teukolsky, S.A., Vetterling, W.T. and Flannery, B.P.: *Numerical Recipes in FORTRAN: The Art of Scientific Computing*(2nd edn.), Cambridge University Press, Cambridge, 1992, pp. 63–78.
[28] Bonner, J.T., Fey, P. and Cox, E.C.: Expression of Prestalk and Prespore Proteins in Minute, Two-Dimensional *Dictyostelium* Slugs, *Mech. Dev.* **88**(1999), 253–254.
[29] Loomis, W.F.: Role of the Surface Sheath in the Control of Morphogenesis in *Dictyostelium Discoideum, Naure New Bio*. **240**(1972), 6–S9.
[30] Inouye, K. and Takeuchi, I.: Analytical Studies on Migrating Movement of the Pseudoplsmodium Of *Dictyostelium Discoideum*, *Protoplasma* **99**(1979), 289–304.
[31] Durston, A.J. and Vork, F.: A Cinematographical Study of the Development of Vitally Stained *Dictyostelium Discoideum*, *J. Cell Sci.* **36**(1979), 261–279.
[32] Shaffer, B.M.: Cell Movement Within Aggregates of the Slime Mould *Dictyostelium Discoideum* Revealed by Surface Markers, *J. Embryol. Exp. Morphol*. **13**(1965), 97–117.